TO BE SUBMITTED
TO NUOVO CIMENTO

CERN/TC/PHYSICS 66-10
7.6.1966

THE REACTION $p\bar{p} \rightarrow N^{*}_{33} \bar{N}^{*}_{33}$ at 5.7 GeV/c

V. Alles-Borelli*, B. French, Å. Frisk, L. Michedja**

CERN, Geneva.

Summary

A study of 3638 events of the reaction $p\bar{p} \rightarrow p\bar{p}\pi^{+}\pi^{-}$ at 5.7 GeV/c in the 81 cm Saclay Hydrogen Bubble Chamber is reported. The measurements were made with the CERN HPD system. The cross section for the channel $p\bar{p} \rightarrow p\bar{p}\pi^{+}\pi^{-}$ was found to be (3.31 ± 0.16)mb. Abundant associated production of $N^{*}_{33}(1238)\ \bar{N}^{*}_{33}(1238)$ has been observed; the cross section for the process $p\bar{p} \rightarrow N^{*}_{33}\ \bar{N}^{*}_{33}$ is (2.08 ± 0.14)mb which corresponds to (63 ± 3) % of the total cross section for the studied channel.

The production mechanism of $N^{*}_{33}\ \bar{N}^{*}_{33}$ has been investigated and the experimental results compared with various predictions of the one pion exchange model modified to take into account absorption in the initial and final states (absorption model). The slope of the differential cross section is rather well reproduced by this model, the experimental value is however exceeded by a factor of about three. The decay parameters of the joint decay distribution have been measured and found to be in a reasonable agreement with the theoretical predictions. A small correlation between the decay angles of the N^{*}_{33} and $\bar{N}^{*}_{33}$ respectively of 0.10 ± 0.04 has been found and is in agreement with the prediction of 0.05 from the absorption model.

---

* Now at the Institute of Physics, Bologna.

** On leave of absence from Institute of Nuclear Research, Warsaw

1. Experimental Procedure

The 81 cm Saclay hydrogen bubble chamber was exposed to a separated beam of 5.7 GeV/c antiprotons from the CERN proton synchrotron. The pion and muon contaminations of the beam were 2 and 6 % respectively. Each frame contained, on average, 14 beam tracks. Four-prong interactions (without accompanying V^o) were selected for measurement with the CERN HPD system. Out of about 21,000 events attempted 19,100 could be successfully reconstructed after a single remeasurement of events which failed in the first pass through the system.

About 900 events of the total sample were also measured with IEP measuring projectors. A comparison of the results obtained with the HPD and with the conventional methods has been made, the details of which are given in Ref. 1. In this comparison sample, those events which were not accepted for physics from the HPD measurements were investigated for any bias with respect to the accepted part. No bias could be detected.

The events were processed through the chain of CERN computer programmes for analysis of bubble chamber pictures. Ionization measurements from the HPD were used together with kinematics in the identification of the events.

Of the many final states which are possible, we have so far studied the following :

$\bar{p}p \rightarrow \pi^+\pi^+\pi^-\pi^-$	(191 events)	(1)
$\bar{p}p \rightarrow p\bar{p}\pi^+\pi^-$	(3638 events)	(2)
$\bar{p}p \rightarrow p\bar{p}\pi^+\pi^-\pi^o$	(2312 events)	(3)
$\bar{p}p \rightarrow pn\pi^+\pi^-\pi^-$ and C.C.	(1584 events)	(4)

Events were considered to belong to the four constraint channel (2) if the kinematical probability ($P\chi^2_{4c}$) was greater than 1 % and if the ionization was in agreement with the chosen hypothesis. For the small number of events which had an ambiguity concerning the negative tracks the fit with the higher probability was chosen.

An investigation of the four pion channel (1) has already been published[2]. The reaction $p\bar{p} \to p\bar{p}\pi^+\pi^-\pi^0$ is treated in a separate paper[3] with the emphasis on the three body final states $p\bar{p}\omega$, $p\bar{p}\eta$ and $N^{*}_{33}\,\bar{N}^{*}_{33}\,\pi^0$. The production of the nucleon isobars $N^{*}(1518)$ and $N^{*}(1688)$ and their decay characteristics has also been studied[4]. In the present paper the reaction $p\bar{p} \to p\bar{p}\pi^+\pi^-$ will be discussed, especially the production mechanism for $N^{*}_{33}\,\bar{N}^{*}_{33}$. This process has been studied previously in the momentum range 3.25 - 7 GeV/c[5-8].

2. Cross-sections

Out of 19,100 events, 3638 fitted the reaction $p\bar{p} \to p\bar{p}\pi^+\pi^-$ giving a cross-section of (3.31 ± 0.16) mb. This agrees well with that of (3.18 ± 0.20) mb obtained by the Bonn-Hamburg-Milan collaboration[7] (hereafter referred to as the B-H-M collaboration) at the same energy. The cross section value was obtained from the total 4-prong cross section (17.3 ± 0.7) mb which was determined from part of the available film. The error consists of the statistical error coming mainly from the total 4-prong cross-section, and the uncertainties due to channel separation.

In Fig. 1 we have plotted a scatter diagram of the invariant masses of the $(p\pi^+)$ and the $(\bar{p}\pi^-)$ systems. The production of N^{*}_{33} and its anti-particle is easily detected as a strong cluster in the overlap region of the two bands centred at a mass value of about 1215 MeV/c^2 on each axis.

In order to estimate the cross section of the $N^{*}_{33}\,\bar{N}^{*}_{33}$ production we assume that the final state can be described with the following non-interfering channels :

a) $p\bar{p} \to N^{*}_{33}\,\bar{N}^{*}_{33}$ (double isobar production)
b) $p\bar{p} \to N^{*}_{33}\,\bar{p}\pi^-$ (single isobar production)
c) $p\bar{p} \to p\pi^+\,\bar{N}^{*}_{33}$ (- " -)
d) $p\bar{p} \to p\pi^+\bar{p}\pi^-$ (non-resonant background)

To determine the relative frequency of each channel (a - d) we followed the procedure of Ferro-Luzzi et al. in their paper on $K^{\pm} N^{\pm}$ - production in K^+p reactions at 3 GeV/c[9]. We do not give the full description of the method here since this is done in the above mentioned paper in a complete way. The resonances are described by a p-wave relativistic Breit-Wigner distribution[10]

$$BW \sim \frac{\Gamma}{(M^2 - M_{N^*}^2)^2 + \Gamma^2 M_{N^*}} \qquad (5)$$

$$\Gamma = \Gamma_{N^*} \frac{q_{p\pi}^3}{q_{p\pi}^3 (M_{N^*})} \cdot \frac{(1 + D_1(M_{N^*}))}{(1 + D_1(M_{p\pi}))} \qquad (6)$$

M_{N^*} and Γ_{N^*} are the intrinsic mass and width of the N^*. $q_{p\pi}$ is the relative momentum between the nucleon and the pion in the $p\pi$ rest frame. The factor D_1 is defined by the equation $D_1 = (q_{p\pi} \cdot r)^2$, r being the interaction radius of the $p\pi$-system. All non-resonant contributions are assumed to follow their phase space. It should be mentioned that we use a different formula to that of Ferro-Luzzi et al. for the energy dependence of the width. Their expression contains a factor of the type

$$\frac{(M_{p\pi} + M_p)^2 - M_\pi^2}{M_{p\pi}^2} \cdot \frac{M_{N^*}^2}{(M_{N^*} + M_p)^2 - M_\pi^2}$$

instead of $\frac{1 + D_1(N^*)}{1 + D_1(M_{p\pi})}$. The former approach is found from lowest order perturbation theory, the latter comes from nuclear reaction theory. A further discussion of this problem is given below.

The distribution function of the events over the kinematically allowed region can be written

$$L = f_{N^{*\pm}N^{*\pm}} \cdot F_{N^{*\pm}N^{*\pm}} + f_{N^{*\pm}} \cdot F_{N^{*\pm}} + f_{\Delta^{*\pm}} \cdot F_{\Delta^{*\pm}} + (1 - f_{N^{*\pm}N^{*\pm}} - f_{N^{*\pm}} - f_{\Delta^{*\pm}}) \cdot F_{pp\pi^+\pi^-} \qquad (7)$$

where the f's are the fractions and F's the distribution functions, i.e. Breit-Wigner functions and phase space of the events for the different channels (a-d).

A likelihood fit was made in order to determine the fractions, the masses and widths of the Breit-Wigner functions and the interaction radius of the $p\pi$ system. This gives a total of 8 parameters. If we invoke charge conjugation the number of parameters reduces to 5. The results of the 8-parameter fit are given in Table I.

Concerning the errors, the following comment has to be made. In all attempts to find a reasonable fit to the data we found that the most sensitive point was the type of the Breit-Wigner function. Using for instance, the same type of formula for the energy dependence of the width as Ferro-Luzzi et al., no acceptable fit could be obtained ($P_{\chi^2} < 0.1$ %). In view of this fact and the uncertainties in some of our assumptions e.g. the phase space behaviour of the non-resonant contributions and the absence of interference, the errors of the fitted parameters should be treated with caution. From the variation of these parameters when using different fitting procedures we find it justified to increase the fitted errors by a factor of two, and it is these enlarged errors that are given in Table I.

The parameters for N^{*}_{33} and $\bar{N}^{*}_{33}$ agree with each other reasonably well. The mass values are however considerably lower than the accepted one of (1236.0 ± 1.5) MeV/c^2[11], which is based on the phase shift analysis of elastic scattering data. In production experiments the mass values and widths vary with the type of reaction and C.M.S. energy and in general the mass value turns out to be lower than the accepted one[9,12]. This fact has been discussed by Jackson[10] who showed that modifications of the Breit-Wigner formula can result in a shift of the fitted mass to a higher value. Had we not used the formula (5) but instead, an s-wave non-relativistic Breit-Wigner, the value of the mass obtained would have been 1215 instead of 1223 MeV/c^2.

A comparison between the measured and fitted distributions shows a systematic excess of events at small masses of the $(p\pi^+)$ and $(\bar{p}\pi^-)$ systems above the fitted distributions (Fig. 2a and b). This discrepancy is what one

might imagine could arise from the peripheral nature of the reactions (a-d). We have tried to account for this by inserting a factor, being essentially a weight to each event according to the four momentum transfer distribution, which modifies the phase space part of the distribution functions. This phase space modification however neither leads to a better fit as judged from a χ^2- test nor gives any considerable changes in the fitted values of the parameters.

The frequency (63 ± 3) % for double production corresponds to a cross section of (2.08 ± 0.14) mb. The cross section for single production is $2 \times (0.33 \pm 0.07)$ mb. The B.H.M collaboration has obtained a cross section for double production of (1.28 ± 0.11) mb[7], which corresponds to all events in the "double isobar region" in that work defined as $1130 < M_{p\pi^+}, M_{p\pi^-} < 1330$ MeV/c^2. According to our fit there is however a considerable contribution (~ 40 %) to the double production cross section coming from outside the so-called double isobar region. In fact what can be distinguished as bands going out from the strongly populated region on Fig. 1 is partly due to double production. Other groups have studied the same reaction at different energies but due to various methods of analysis it is difficult to extract reliable information on the variation of the $N^*_{33}\,\bar{N}^*_{33}$ cross section with energy. Thus at lower energies Ferbel et al.[5] obtain $\sigma(p\bar{p} \to p\bar{p}\pi^+\pi^-) = (3.43 \pm 0.23)$ mb at 3.28 GeV/c and (3.67 ± 0.30) mb at 3.66 GeV/c. The frequency of double production was found to be about 80 % and corresponds to a cross section of 2.8 mb, where the figure of 80 % was obtained by comparing the data with various admixtures of phase space and s-wave Breit-Wigner resonant functions. The result of Dehne et al.[6] at 3.60 GeV/c is $\sigma(p\bar{p} \to p\bar{p}\pi^+\pi^-) = (3.81 \pm 0.23)$ mb with a double production cross section of (2.13 ± 0.13) mb or 56 % of the total $p\bar{p}\pi^+\pi^-$ cross section. These figures are based on counting events in a certain "double isobar region" defined as $1130 < M_{p\pi^+}, M_{p\pi^-} < 1330$ MeV/c^2. At 6.94 GeV/c Ferbel et al.[8] claim that double production can account for about 50 % of the reaction $p\bar{p} \to p\bar{p}\pi^+\pi^-$, the cross section of which is (3.0 ± 0.7) mb. Thus due to the different methods of analysis it is clearly difficult to extract reliable information on the variation of the $N^*_{33}\,\bar{N}^*_{33}$ cross section with energy.

3. Production mechanism of the reaction $p\bar{p} \rightarrow N^{*}_{33} \bar{N}^{*}_{33}$

3.1. Production angular distribution

For the detailed study of the production mechanism of $N^{*}_{33} \bar{N}^{*}_{33}$ we define the double isobar region in the following way : $1150 < M_{p\pi^+}, M_{\bar{p}\pi^-} < 1350$ MeV/c^2. This region contains 1404 events, 94 % of which are due to double production, the rest being 5 % single production and 1 % non-resonant background. The production angular distribution for the $N^{*}_{33} \bar{N}^{*}_{33}$ events shows the typical peripheral feature, N^{*} being sharply peaked forward in the direction of the proton, $\bar{N}^{*}$ backward in the direction of the incident antiproton. In the following sections we compare the experimental distributions with various predictions of the absorption model.

3.2. t-distribution

Fig. 3 shows the t-distribution for the events in the double isobar region, t being the four momentum transfer from the proton to the $(p\pi^+)$ system (or from the antiproton to the $(\bar{p}\pi^-)$ system). The dotted line indicates the corrected experimental distribution after taking into account the fact that 40 % of the contribution to the process $p\bar{p} \rightarrow N^{*}_{33} \bar{N}^{*}_{33}$ comes from outside the double isobar region defined in the text.

Following the theory of Gottfried and Jackson[13], Svensson[14] has calculated the effect on the differential cross section for $p\bar{p} \rightarrow N^{*}_{33} \bar{N}^{*}_{33}$ of the absorption in the initial and final state due to competition from other open channels. The full curve on Fig. 3 shows the absorption model prediction. This model reproduces rather well the slope of the differential cross section. The experimental value is however exceeded by a factor of about 3. The absorption model also predicts the energy variation of the total cross section. However, as mentioned above, the experimental situation is somewhat confused and does not warrant comparison with theory.

Finally it should be remarked that the absolute value of the slope of the t-distribution for the reaction $p\bar{p} \to N^{*}_{33}\,\bar{N}^{*}_{33}$ is considerably smaller than that of the corresponding elastic reaction i.e. for $p\bar{p} \to p\bar{p}$. Our best fit value of $-(6.0 \pm 0.3)\ (\mathrm{GeV/c})^{-2}$ is found by fitting a distribution of the type $F(t) = A\, e^{-Bt}$ to the data of Fig. 3 in the t-interval $0.125 < -t < 0.5\ (\mathrm{GeV/c})^2$. The slope limit corresponds to $-t_{min}$ for $M_{p\pi^+} = M_{\bar{p}\pi^-} = 1350\ \mathrm{MeV/c^2}$. The slope for the elastic reaction is $-(12.0 \pm 0.4)\ (\mathrm{GeV/c})^2$ at 5.7 GeV/c. incident momentum in the -t-interval $0.015 - 0.285\ (\mathrm{GeV/c})^2$ [15]. This result is in contrast to the observation[16,17] that for many quasi two-body reactions the slope turns out to be about the same as for the corresponding elastic reaction.

3.3. Decay angular distribution

The decay angular distribution of a 3/2 isobar decaying into a nucleon and a pion can be written, in a model independent manner, as

$$W(\cos\Theta, \Phi) = \frac{3}{4\pi}\Big[\frac{1}{6}(3 - 4\rho_{11}) - \frac{1}{2}(1 - 4\rho_{11})\cos^2\Theta - \frac{2}{\sqrt{3}}\,\mathrm{Re}\,\rho_{3,-1}\sin^2\Theta\cos 2\Phi - \frac{2}{\sqrt{3}}\,\mathrm{Re}\,\rho_{3,1}\sin 2\Theta\cos\Phi\Big] \qquad (10)$$

where Θ and Φ which are defined in the isobar C.o.M. are the angles introduced by Jackson (Fig. 4). Φ is equivalent to the Treiman-Yang angle. The quantities ρ_{11}, $\mathrm{Re}\,\rho_{3,-1}$ and $\mathrm{Re}\,\rho_{3,1}$ are matrix elements of the spin density matrix, with indices of the type 2 m, 2m', where m and m' are magnetic quantum numbers. These so-called decay parameters can be determined from the experimental distributions of Θ and Φ. A straightforward way of doing this is to integrate over the angles Θ or Φ making use of the fact that the angular functions in (8) are orthogonal so the decay parameters can be evaluated as experimental mean values, for example we find for the N^{*}_{33} with the decay angles Θ and Φ (and the same for $\bar{N}^{*}_{33}$ with $\bar{\Theta}$ and $\bar{\Phi}$)

$$\rho_{11} = \frac{15}{8}\langle \cos^2\theta \rangle - \frac{3}{8} \qquad (9)$$

$$\mathrm{Re}\ \rho_{3,-1} = -\frac{5\sqrt{3}}{8}\langle \sin^2\theta \cos^2\Phi \rangle \qquad (10)$$

$$\mathrm{Re}\ \rho_{3,1} = -\frac{5\sqrt{3}}{8}\langle \sin^2\theta \cos\Phi \rangle \qquad (11)$$

The unmodified one pion exchange model predicts $\rho_{11} = 0.5$, $\mathrm{Re}\ \rho_{3,-1} = 0$ and $\mathrm{Re}\ \rho_{3,1} = 0$ which corresponds to a distribution in $\cos\theta$ of the type $1 + 3\cos^2\theta$ and an isotropic distribution in Φ. The corrections for the decay parameters introduced by the absorption model have been calculated by Svensson[14]. Fig. 5 (a,b,c) shows the experimental values in the double isobar region. We have invoked charge conjugation and taken the average for N^{*}_{33} and $\bar{N}^{*}_{33}$. The solid curves represent the predictions of the absorption model. The experimental values have been corrected for the influence of the background by evaluating the parameters in a control region, 70 MeV/c^2 wide, surrounding the double isobar square. In most cases the correction could be neglected.

Fig. 6a shows the distribution of $\cos\theta$ and $\cos\bar{\theta}$, Fig. 6b that of Φ and $\bar{\Phi}$ for all events in the double isobar region. The shaded parts of the plots represent events not corresponding to double production, and have been subtracted from the total sample. The shape of this background has been obtained from studies in the control region. The solid curve on Fig. 6a represents the best fit of the distribution function

$$W(\cos\theta) = \frac{3}{2}\left[\frac{1}{6}(3 - 4\rho_{11}) - \frac{1}{2}(1 - 4\rho_{11})\cos^2\theta\right] \qquad (12)$$

with a fitted value of $\rho_{11} = 0.34 \pm 0.01$. The fit turns out to be good, the probability P_{χ^2} being about 50 %. The value of the ρ_{11} -parameter agrees with the average value of ρ_{11} for all t-intervals calculated with the formula (9). $W(\cos\theta)$ (formula 12) with $\rho_{11} = 0.34$ corresponds to a distribution in $\cos\theta$ of the type $1 + A\cos^2\theta$ with $A = 0.65$. Thus the effect of the absorption in the initial and final state of the reaction $p\bar{p} \rightarrow N^{*}_{33}\,\bar{N}^{*}_{33}$ is to reduce A from 3 to 0.65. The distribution of Φ and $\bar{\Phi}$ (Fig. 6b) is consistent with isotropy.

Pilkuhn and Svensson[18] have pointed out that by using the joint decay distribution $W(\cos\Theta, \cos\bar{\Theta}, \Phi, \bar{\Phi})$ of N^{*}_{33} and $\bar{N}^{*}_{33}$ one can extract more information than by studying each decay separately: the latter method gives, as can be seen from equations 9 - 11 above, 6 parameters, 3 for each decay while the former procedure gives 13 additional parameters. These may be evaluated in the same way as the separate parameters. The formulae are given in appendix I. The experimental data and theoretical predictions from the absorption model are shown in Fig. 5(d-l). The overall agreement is good but the experimental errors are obviously too large to allow a serious test of the model with these parameters. The unmodified one pion exchange model predicts that the parameters on Fig. 5 (d-k) are equal to zero except for the last one Fig. 5 (l), which is expected to be $\frac{1}{4}$.

A further prediction of the absorption model is the existence of a correlation between the decays of the N^{*}_{33} and the $\bar{N}^{*}_{33}$ in the decay angles Θ and $\bar{\Theta}$. By making a likelihood fit of the joint decay distribution of $\cos\Theta$ and $\cos\bar{\Theta}$ the correlation parameter has been determined for different t-intervals. The joint decay distribution may be written

$$W(\cos\Theta, \cos\bar{\Theta}) = \frac{1}{4}\Big[\{1 + (1 - 3\cos^2\Theta)a\}\{1 + (1 - 3\cos^2\bar{\Theta})a\} + (1 - 3\cos^2\Theta)(1 - 3\cos^2\bar{\Theta})(b - a^2)\Big] \quad (13)$$

with $a = \frac{1}{2} - 2\rho_{11}$ (14)

and $b = \frac{1}{2}(\rho^{33}_{--} - \rho^{11}_{--})$ (15)

ρ^{33}_{--} and ρ^{11}_{--} are functions of certain matrix elements of the joint spin density matrix[18]. The absence of a correlation between the decays of the N^{*}_{33} and $\bar{N}^{*}_{33}$ would mean that the joint decay distribution in $\cos\Theta$ and $\cos\bar{\Theta}$ can be written as a product of the simple distributions (formula 12 with $\rho_{11} = \frac{1}{4} - \frac{1}{2}a$ for $\cos\Theta$ and $\cos\bar{\Theta}$ respectively). The condition for this is obviously $b - a^2 = 0$. The value of the correlation parameter $b - a^2$ for different t-intervals is shown in Fig. 7. The prediction of the absorption model is 0.05 for all production angles. Our mean value over the whole

t-range is 0.10 ± 0.04, which supports the observation made by other groups[13] and is in agreement with the prediction of the absorption model.

Conclusions

I. The cross section for the reaction $p\bar{p} \rightarrow p\bar{p}\pi^+\pi^-$ at 5.7 GeV/c is found to be (3.31 ± 0.16) mb. An abundant production of N^*_{33} in pair with its anti-particle has been observed; the cross section for the process $p\bar{p} \rightarrow N^*_{33}\,\bar{N}^*_{33}$ is (2.08 ± 0.14) mb which corresponds to (63 ± 3) % of the total cross section for the studied reaction. The single production cross section is (0.66 ± 0.14) mb.

The Breit-Wigner fit of the N^*_{33} and $\bar{N}^*_{33}$ gave the following results :

$$M_{N^*} = (1221 \pm 3)\ \text{MeV/c}^2\ ; \quad \Gamma_{N^*} = (104 \pm 9)\ \text{MeV/c}^2$$

$$M_{\bar{N}^*} = (1224 \pm 3)\ \text{MeV/c}^2\ ; \quad \Gamma_{\bar{N}^*} = (117 \pm 11)\ \text{MeV/c}^2\ .$$

II. The one pion exchange model, modified to take into account absorption in the initial and final states is able to reproduce fairly well the slope of the differential cross section for the reaction $p\bar{p} \rightarrow N^*_{33}\,\bar{N}^*_{33}$, the experimental value is however exceeded by a factor of about three. Concerning the energy variation of the total cross section, the experimental situation is unclear.

III. The decay parameters of the joint decay distribution have been measured and found to be in reasonable agreement with the theoretical predictions of the absorption model. However, only a few parameters e.g. ρ_{11}, Re $\rho_{3,1}$ and Re $\rho_{3,-1}$ have small enough errors to allow a serious test of the model. For ρ_{11} the deviation from 0.5 (which is the prediction of the unmodified one pion exchange model) is statistically significant and in fair agreement with the absorption model.

IV. A small correlation between the decays of N^*_{33} and $\bar{N}^*_{33}$ in the decay angles Θ and $\bar{\Theta}$ has been observed. The experimental value for the correlation parameter $(b - a^2)$ is 0.10 ± 0.04 which agrees with the prediction of 0.05 from the absorption model.

Acknowledgements

We would like to express our thanks to the operating groups of the CERN proton synchrotron and the 81 cm Saclay bubble chamber. We are grateful to Drs. A. Accensi, J.M. Howie, W. Krischer, W.G. Moorhead, B.W. Powell, P. Seyboth and P. Villemoes for their important work during various parts of the automatic processing of the data. Thanks are due to Drs. H. Pilkuhn, B.E.Y. Svensson and K. Zalewski for many valuable discussions on certain theoretical problems. It is a pleasure to acknowledge the help given to us by Dr. G. Sheppey. We thank Dr. R. Armenteros and Prof. Ch. Peyrou for support and clarifying discussions.

APPENDIX I

Formulae for the joint decays parameters. For notations see ref. 18.

$$\mathrm{Re}\,(\rho^{3,-1}_{3,-1} + \rho^{1,-3}_{3,-1}) = \frac{3}{2}\,\langle \cos 2\,(\bar{\Phi} + \bar{\bar{\Phi}})\rangle \qquad (A1)$$

$$\mathrm{Re}\,(\rho^{3,-1}_{-1,3} + \rho^{1,-3}_{-1,3}) = \frac{3}{2}\,\langle \cos 2\,(\bar{\Phi} - \bar{\bar{\Phi}})\rangle \qquad (A2)$$

$$\mathrm{Re}\,\rho^{3,-1} = -\frac{5\sqrt{3}}{4}\,\langle \cos 2\,\bar{\bar{\Phi}}\,(1 - 3\cos^2\theta)\rangle \qquad (A3)$$

$$\mathrm{Re}\,\rho_{3,-1} = -\frac{5\sqrt{3}}{4}\,\langle \cos 2\,\bar{\Phi}\,(1 - 3\cos^2\bar{\theta})\rangle \qquad (A4)$$

$$\mathrm{Re}\,\rho^{3,1} = -\frac{25\sqrt{3}}{16}\,\langle (1 - 3\cos^2\bar{\theta})\,\sin 2\theta\,\cos\bar{\bar{\Phi}}\rangle \qquad (A5)$$

$$\mathrm{Re}\,\rho_{3,1} = -\frac{25\sqrt{3}}{16}\,\langle (1 - 3\cos^2\theta)\,\sin 2\bar{\theta}\,\cos\bar{\Phi}\rangle \qquad (A6)$$

$$\mathrm{Re}\,(\rho^{3,1}_{3,1} - \rho^{-1,-3}_{3,1}) = \frac{225}{48}\,\langle \sin 2\theta\ \sin 2\bar{\theta}\ \cos(\bar{\Phi} + \bar{\bar{\Phi}})\rangle \qquad (A7)$$

$$\mathrm{Re}\,(\rho^{3,1}_{1,3} - \rho^{-1,-3}_{1,3}) = \frac{225}{48}\,\langle \sin 2\theta\ \sin 2\bar{\theta}\ \cos(\bar{\Phi} - \bar{\bar{\Phi}})\rangle \qquad (A8)$$

$$\mathrm{Re}\,(\rho^{3,-1}_{3,1} + \rho^{1,-3}_{3,1}) = \frac{225}{48}\,\langle \sin 2\theta\ \sin 2\theta\ \cos(2\bar{\Phi} + \bar{\bar{\Phi}})\rangle \qquad (A9)$$

$$\mathrm{Re}\,(\rho^{3,1}_{3,-1} + \rho^{3,1}_{1,-3}) = \frac{225}{48}\,\langle \sin 2\bar{\theta}\ \sin 2\theta\ \cos(2\bar{\bar{\Phi}} + \bar{\Phi})\rangle \qquad (A10)$$

$$\mathrm{Re}\,(\rho^{3,-1}_{1,3} + \rho^{1,-3}_{1,3}) = \frac{225}{48}\,\langle \sin 2\theta\ \sin 2\bar{\theta}\ \cos(2\bar{\Phi} - \bar{\bar{\Phi}})\rangle \qquad (A11)$$

$$\mathrm{Re}\,(\rho^{1,3}_{3,-1} + \rho^{1,3}_{1,-3}) = \frac{225}{48}\,\langle \sin 2\bar{\theta}\ \sin 2\theta\ \cos(\bar{\Phi} - 2\bar{\bar{\Phi}})\rangle \qquad (A12)$$

$$\frac{1}{2}\,(\rho^{3,3} - \rho^{1,1}) = \frac{100}{64}\,\langle (1 - 3\cos^2\theta)\,(1 - 3\cos^2\bar{\theta})\rangle \qquad (A13)$$

TABLE I

Parameter	Fitted Value
$M_{N^{*}}$	(1221 ± 3) MeV/c^2
$\Gamma_{N^{*}}$	(104 ± 9) MeV/c^2
$M_{\bar{N}^{*}}$	(1224 ± 3) MeV/c^2
$\Gamma_{\bar{N}^{*}}$	(117 ± 11) MeV/c^2
$f_{N^{*}}$	(11 ± 2) %
$f_{\bar{N}^{*}}$	(10 ± 2) %
$f_{N^{*}\bar{N}^{*}}$	(63 ± 3) %
r	(1.9 ± 0.5) Fermi

$\chi^2 = 46$ for 34 degrees of freedom. ($p_{\chi^2} \sim 10$ %)

N.B. as mentioned in the text, the quoted errors are twice those found from the fit procedure.

REFERENCES

1) P. Villemoes, CERN Yellow Report 66-4. (See also A. Accensi, V. Alles-Borelli, B. French, Å. Frisk, J.M. Howie, L. Michejda, W.G. Moorhead, B.W. Powell, V. Villmoes, Proceedings of the Conference on Programming for Flying Spot Devices at Columbia University, October 1965).

2) A. Accensi, V. Alles-Borelli, B. French, Å. Frisk, J.M. Howie, W. Krischer, L. Michejda, W.G. Moorhead, B.W. Powell, P. Seyboth, P. Villemoes, Phys. Letters 20, 557 (1966).

3) V. Alles-Borelli, B. French, Å. Frisk, L. Michejda, CERN/TC/PHYSICS 66-6.

4) V. Alles-Borelli, B. French, Å. Frisk, L. Michejda, CERN/TC/PHYSICS 66-11.

5) T. Ferbel, A. Firestone, J. Sandweiss, H.D. Taft, M. Gailloud, J.W. Morris, W.J. Willis, A.H. Bachman, P. Baumel, R.M. Lea, Phys. Rev. 138 B, 1528 (1965).

6) H.C. Dehne, E. Lohrmann, E. Raubold, P. Söding, M.W. Teucher, G. Wolff, Phys. Rev. 136 B, 843 (1964).

7) K. Böckmann, B. Nellen, E. Paul, J. Borecka, J. Diaz, M. Heeren, M. Liebermeister, E. Lohrmann, E. Raubold, P. Söding, S. Wolff, S. Coletti, J. Kidd, L. Mandelli, V. Pelosi, S. Ratti, L. Tallone, Phys. Letters 15, 356 (1965).

8) T. Ferbel, A. Firestone, J. Johnson, H. Kraybill, J. Sandweiss, H.D. Taft, Nuovo Cimento 38, 19 (1965).

9) M. Ferro-Luzzi, R. George, Y. Goldschmidt-Clermont, V.P. Henri, B. Jongejans, D.W.G. Leith, G.R. Lynch, F. Muller, J.M. Perreau, Nuovo Cimento 39, 417 (1965).

10) J.D. Jackson, Nuovo Cimento 34, 1644 (1964).

11) A.H. Rosenfeld, A. Barbaro-Galtieri, W.H. Barkas, P.L. Bastien, J. Kerz, M. Roos, UCRL - 8030 (1965).

12) E. Boldt, J. Duboc, N.H. Duong, P. Eberhard, R. George, V.P. Henri, F. Levy, J. Poyen, M. Pripstein, J.Crussard, A. Tran, Phys. Rev. 133 B, 220 (1964).

13) K. Gottfried, J.D. Jackson, Nuovo Cimento 34, 735 (1964).

14) B.E.Y. Svensson, Nuovo Cimento, 39, 667 (1965).

/...

REFERENCES (contd.)

15) K. Böckmann, B. Nellen, E. Paul, B. Wagini, I. Borecka, J. Diaz, M. Heeren, M. Liebermeister, E. Lohrmann, E. Raubold, P. Söding, S.S. Wolff, J. Kidd, L. Mandelli, L. Mosca, V. Pelosi, S. Ratti, L. Tallone, Nuovo Cimento 42, 954 (1966).

16) A. Bialas, Phys. Letters 19, 604 (1965).

17) M. Deutschmann, D. Kropp, R. Schulte, H. Weber, W. Woischnig, C. Grote, J. Klugow, H.W. Meier, A. Pose, S. Brandt, V.T. Cocconi, O. Czyzewski, P.F. Dalpiaz, E. Flaminio, H. Hromadnik, G. Kellner, D.R.O. Morrison, S. Nowak, Phys. Letters 19, 608 (1965).

18) H. Pilkuhn, B.E.Y. Svensson, Nuovo Cimento 38, 518 (1965).

FIGURE CAPTIONS

Fig. 1. Scatter diagram of the invariant masses of the $(p\ \pi^+)$ and $(\bar{p}\ \pi^-)$ systems.

Fig. 2a. The experimental and fitted distributions of the $(p\ \pi^+)$ system. The curve a) is the total distribution. The curves b) - e) show the contributions from double production, single production $N^{*}_{33}\bar{p}\ \pi^-$ and $p\pi^+\bar{N}^{*}_{33}$ and non-resonant background respectively. The fitted mass and width of the peak is (1221 ± 3) MeV/c^2 and (104 ± 9) MeV/c^2.

Fig. 2b. The experimental and fitted distributions of the $(\bar{p}\ \pi^-)$ system. The mass and width given by the fit is (1224 ± 3) MeV/c^2 and (117 ± 11) MeV/c^2.

Fig. 3. t-distribution for all events in the double isobar region defined as $1150 < Mp\pi^+, M\bar{p}\pi^- < 1350$ MeV/c^2. The dotted line indicates the corrected differential cross section accounting for the fact that 40 % of the double production comes from outside the double isobar square. The full curve shows the prediction from the absorption model.

Fig. 4. Diagram showing the definitions of the angles Θ and Φ in the rest frame of N^{*}_{33} $(\bar{N}^{*}_{33})$. The Z-axis is along the direction of the beam or target particles and the Y-axis is the production normal defined as $\underset{\sim}{p}_{\bar{p},CM} \times \underset{\sim}{p}_{\bar{N}^{*},CM}$.

Fig. 5a-l. The decay parameters of the joint decay distribution with experimental points for different t-intervals. The curves show the predictions of the absorption model.

Fig. 6a. The cos Θ distribution for all events in the double isobar region. The curve is the best fit curve of the decay angular distribution (12) with $\rho_{11} = 0.34$. The shaded part shows the background events.

Fig. 6b. The distribution of the Treiman-Yang angle for all events in the double isobar region. The background is indicated with the shaded part of the diagram.

Fig. 7. The correlation parameter $b - a^2$ for different t-intervals. The straight line shows the prediction of the absorption model.

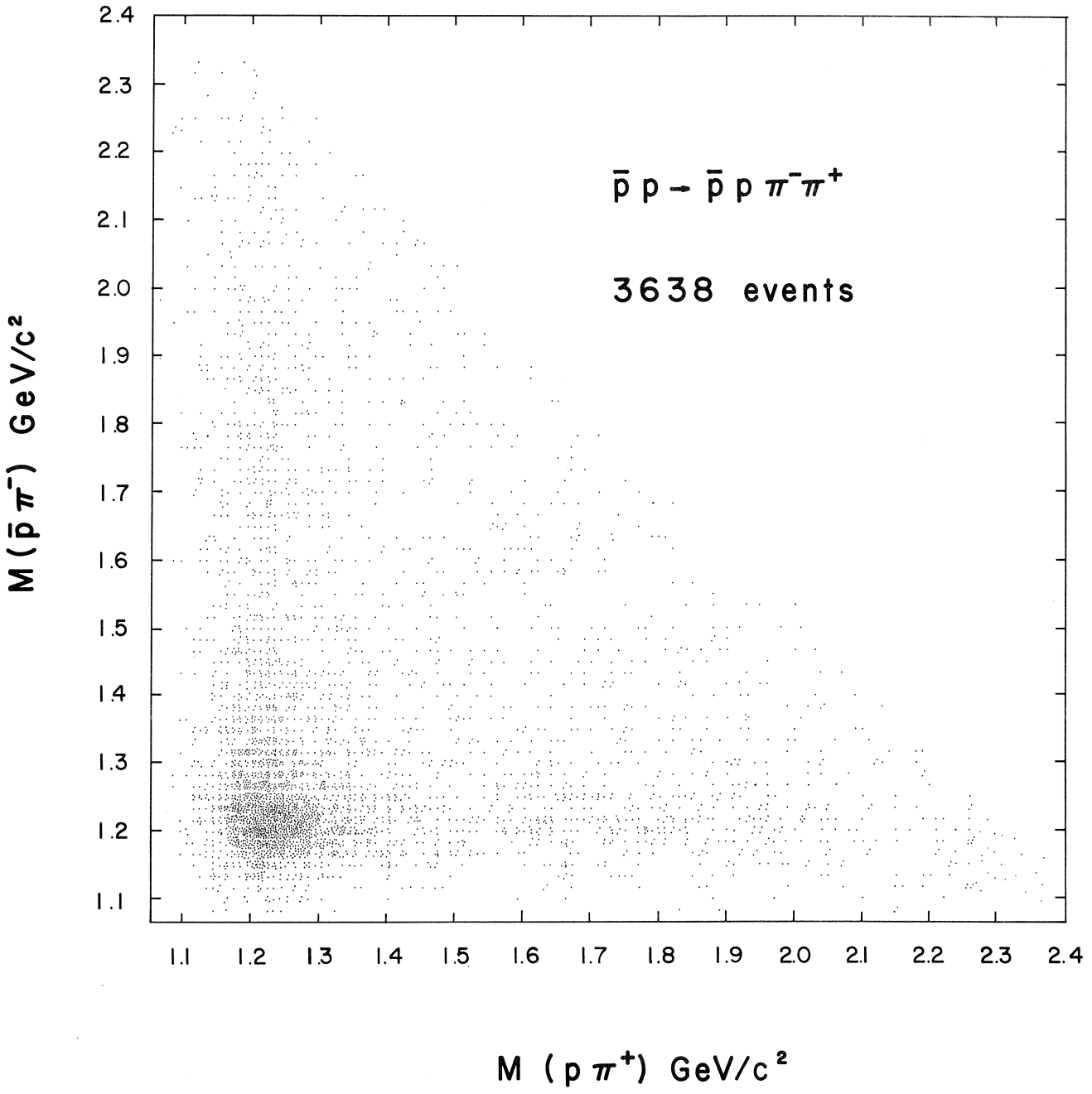
$\bar{p}\,p \to \bar{p}\,p\,\pi^-\pi^+$
3638 events
$M(\bar{p}\pi^-)$ GeV/c²
$M(p\pi^+)$ GeV/c²
2.4
2.3
2.2
2.1
2.0
1.9
1.8
1.7
1.6
1.5
1.4
1.3
1.2
1.1
1.1 1.2 1.3 1.4 1.5 1.6 1.7 1.8 1.9 2.0 2.1 2.2 2.3 2.4

Fig. 1

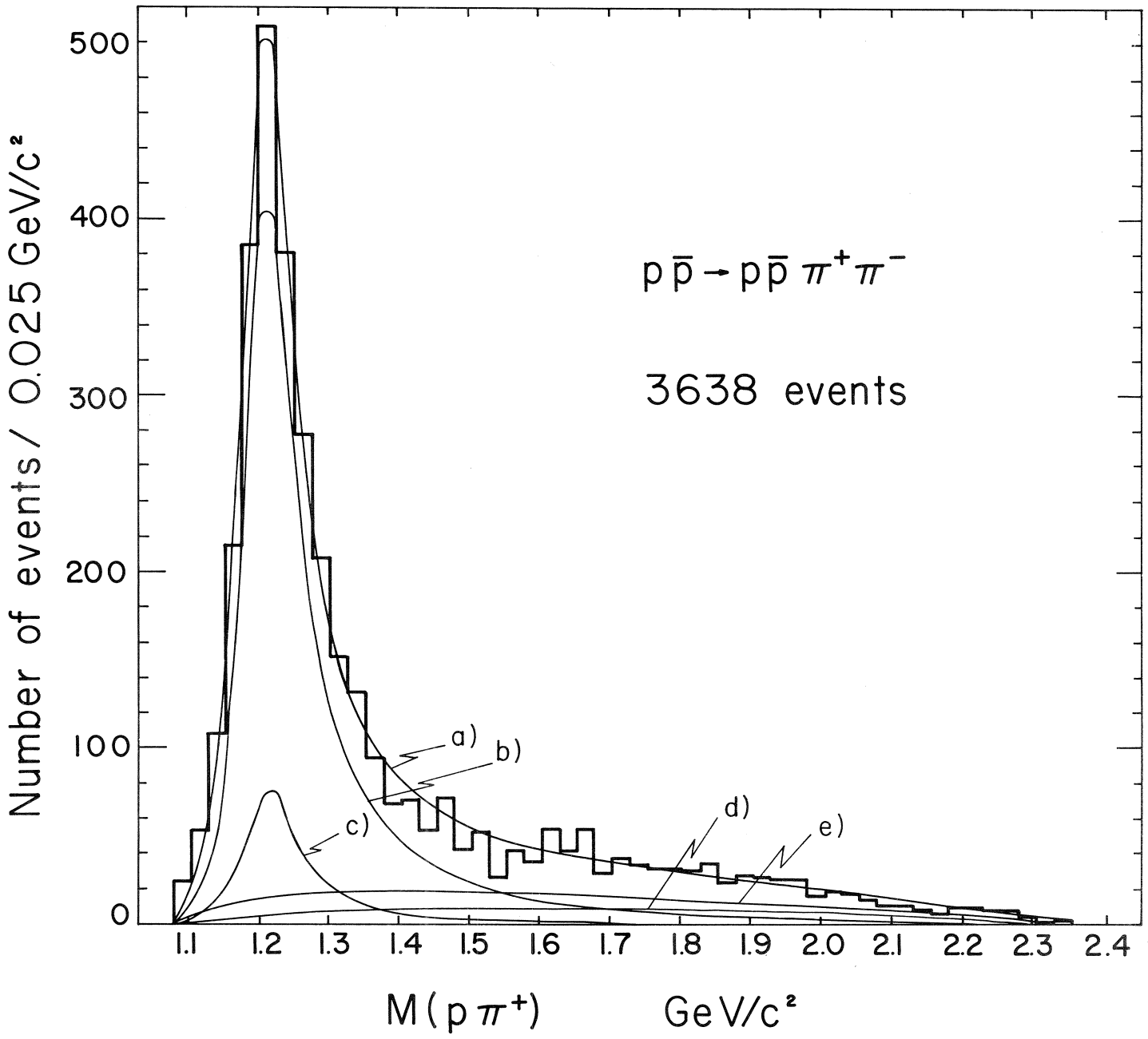
Number of events / 0.025 GeV/c²
500
400
300
200
100
0
1.1
1.2
1.3
1.4
1.5
1.6
1.7
1.8
1.9
2.0
2.1
2.2
2.3
2.4
M(pπ⁺) GeV/c²
pp̄ → pp̄ π⁺π⁻
3638 events
a)
b)
c)
d)
e)

Fig. 2a

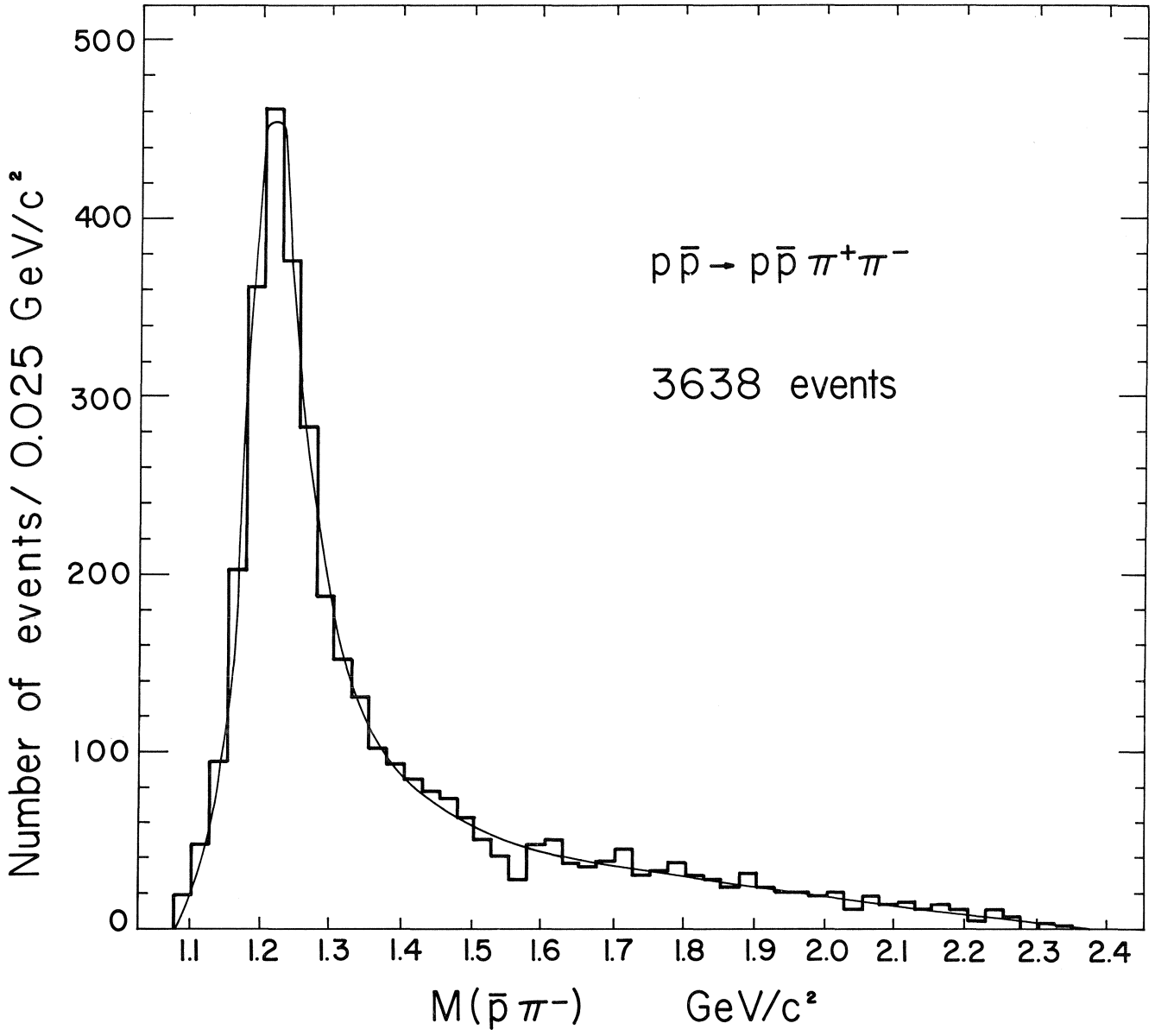
500
400
300
200
100
0
Number of events/ 0.025 GeV/c²
pp̄ → pp̄ π⁺π⁻
3638 events
1.1
1.2
1.3
1.4
1.5
1.6
1.7
1.8
1.9
2.0
2.1
2.2
2.3
2.4
M(p̄ π⁻) GeV/c²

Fig. 2b

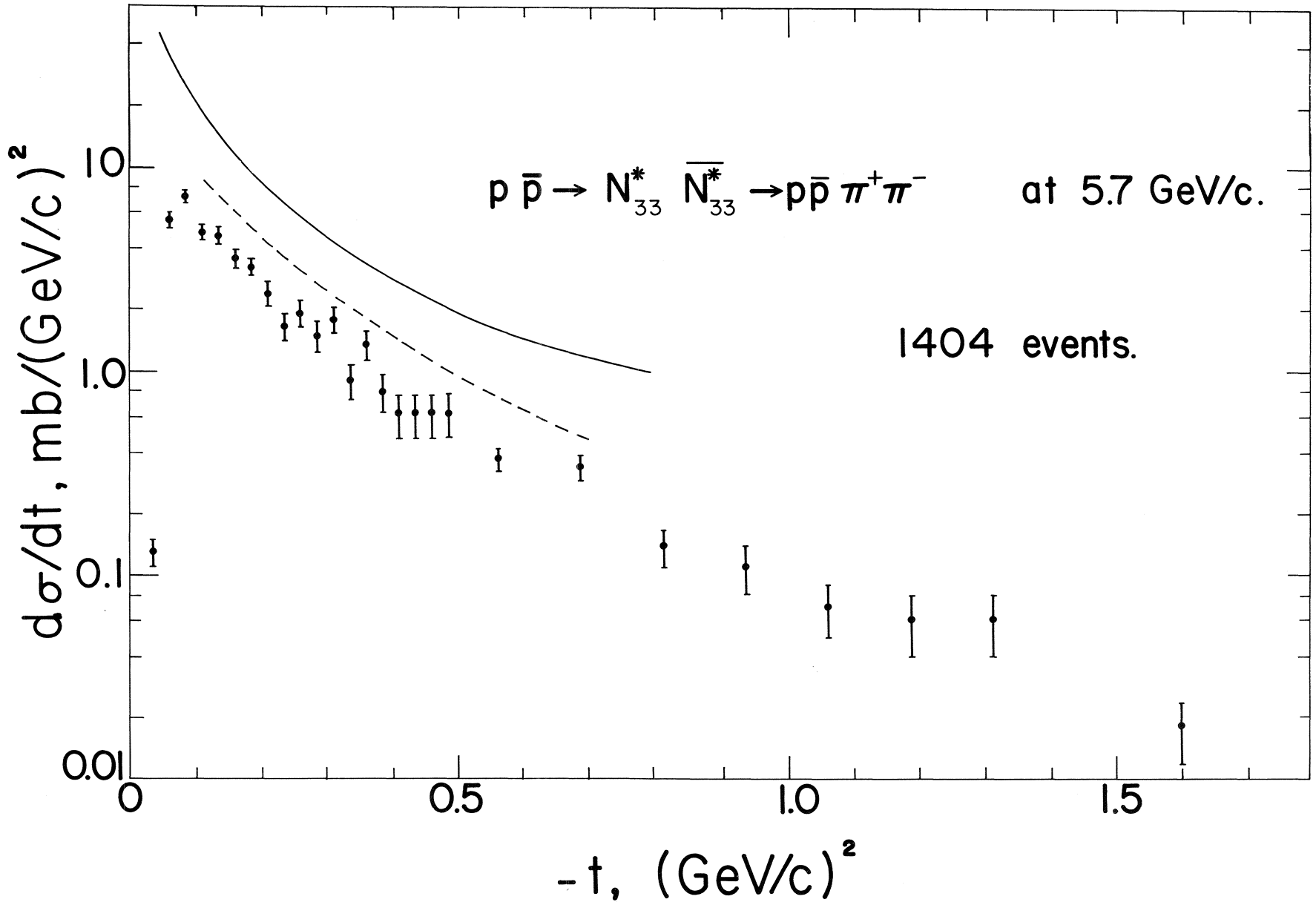
$p\bar{p} \rightarrow N^*_{33}\ \overline{N^*_{33}} \rightarrow p\bar{p}\pi^+\pi^-$ at 5.7 GeV/c.
1404 events.
$d\sigma/dt$, mb/(GeV/c)^2
10
1.0
0.1
0.01
0
0.5
1.0
1.5
$-t$, (GeV/c)^2

Fig. 3

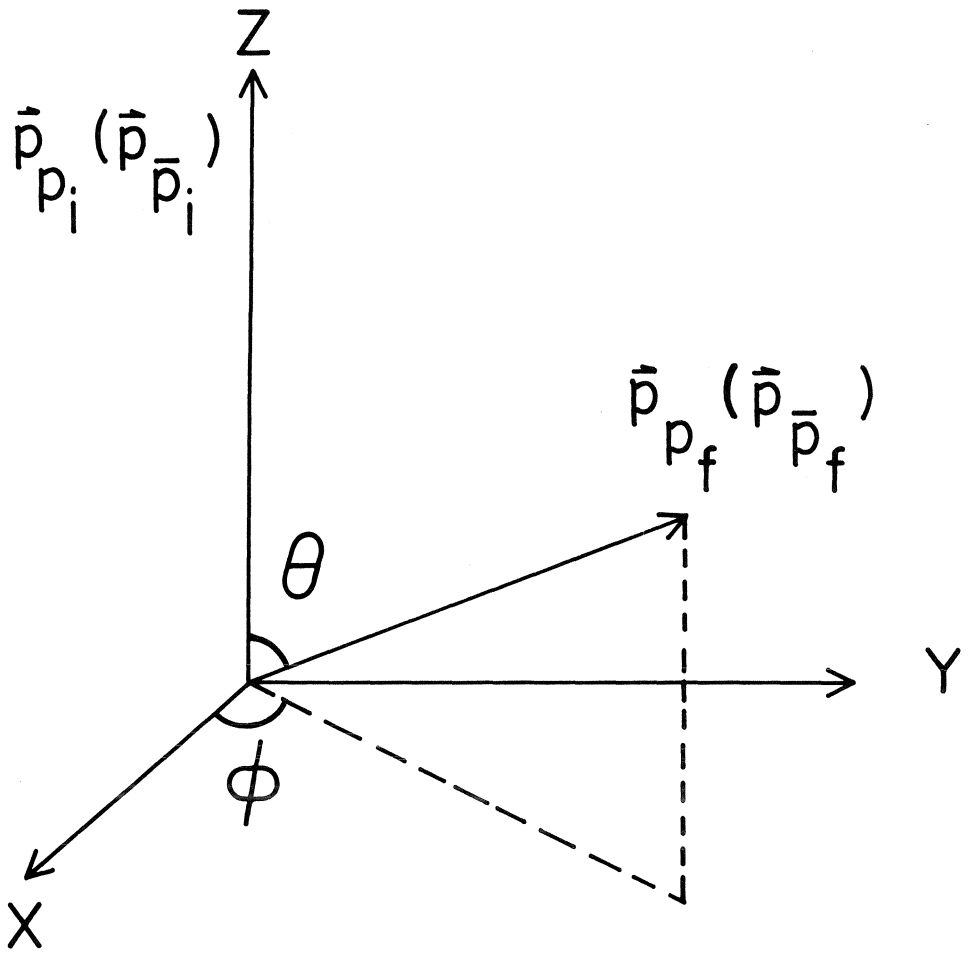

Fig. 4

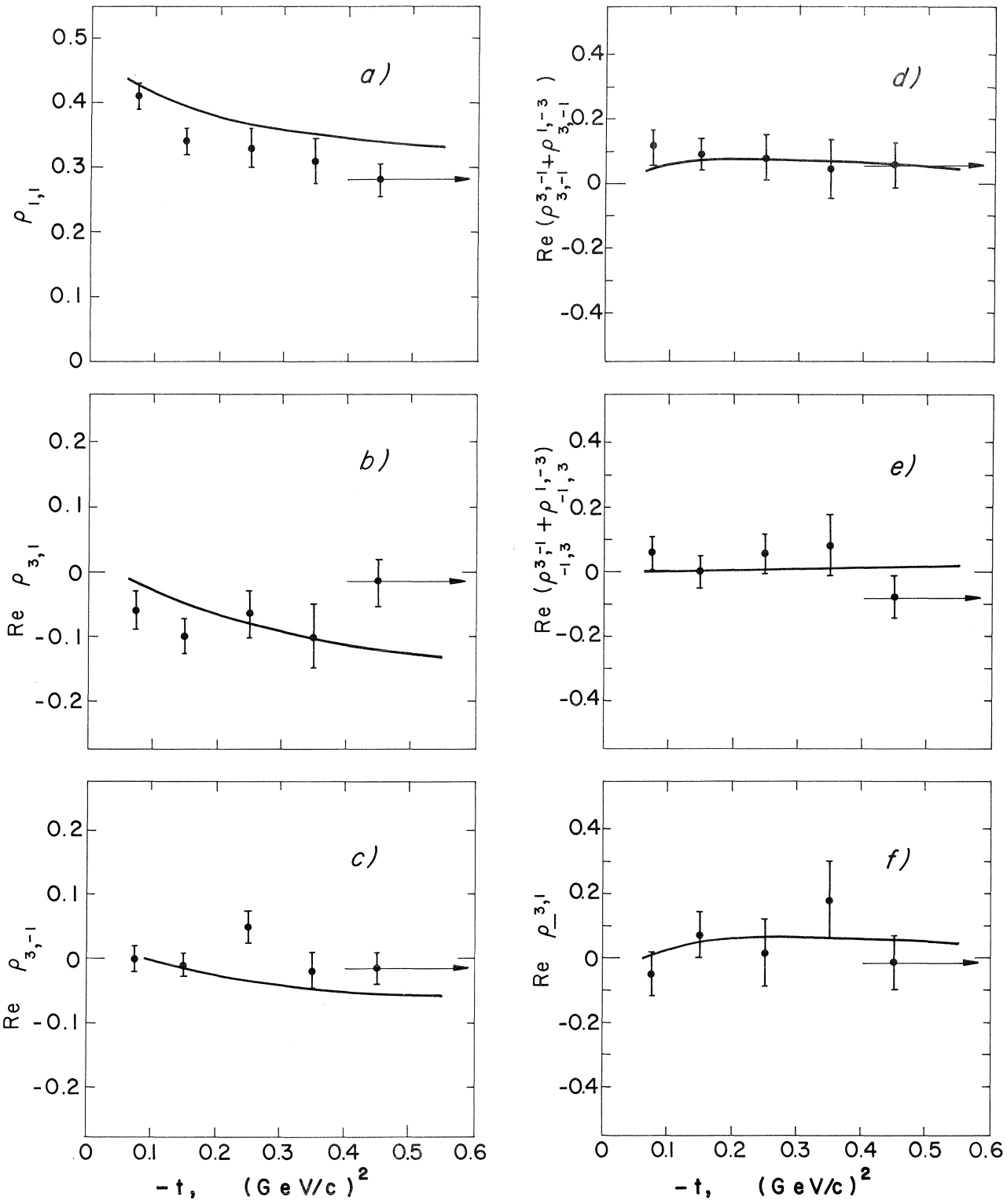
a)
b)
c)
d)
e)
f)
$\rho_{1,1}$
Re $\rho_{3,1}$
Re $\rho_{3,-1}$
Re $(\rho^{3,-1}_{3,-1}+\rho^{1,-3}_{3,-1})$
Re $(\rho^{3,-1}_{-1,3}+\rho^{1,-3}_{-1,3})$
Re $\rho^{3,1}_{-}$
$-t$, (GeV/c)^2
$-t$, (GeV/c)^2

Fig. 5a-f

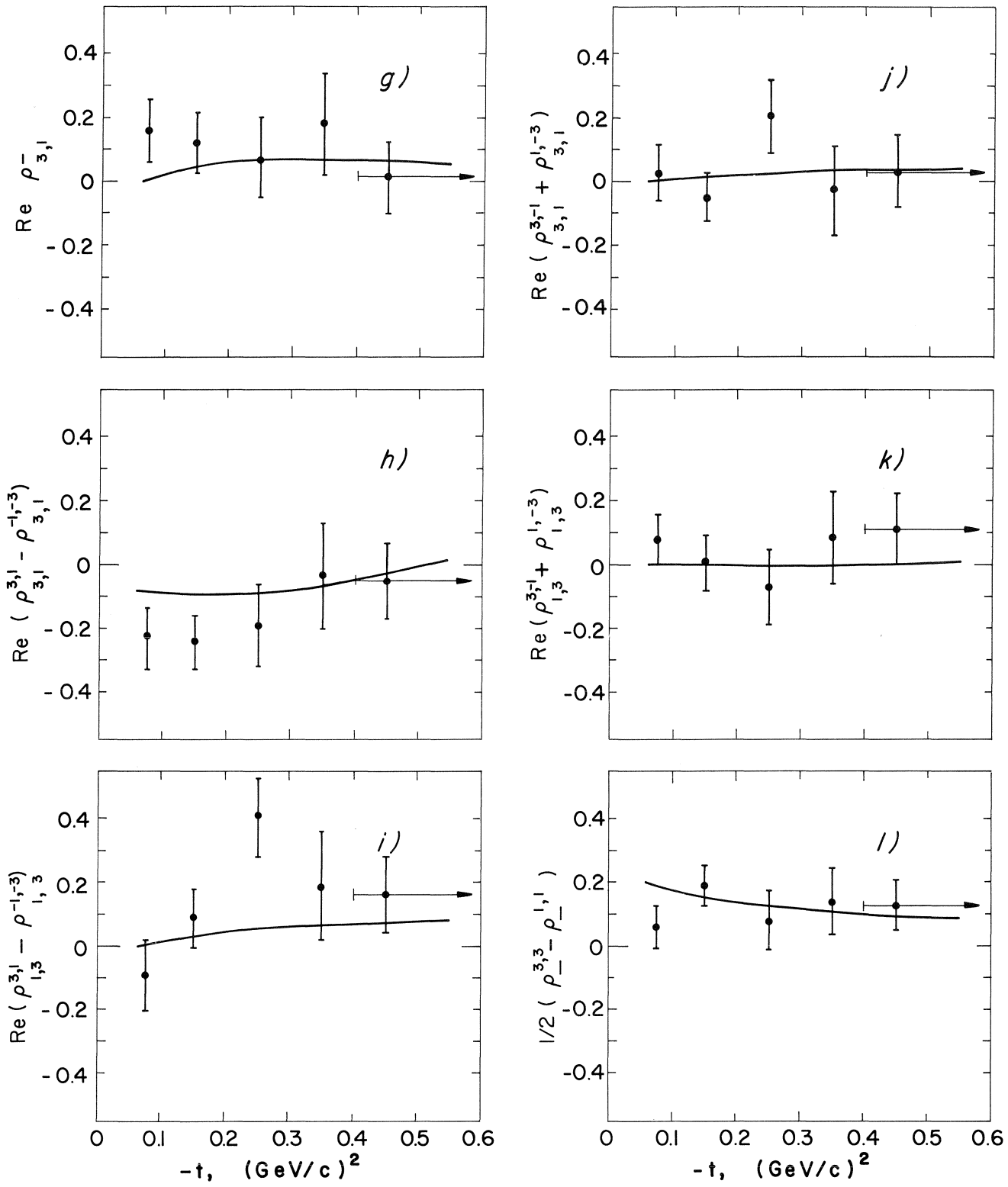
g)
h)
i)
j)
k)
l)
Re $\rho^{-}_{3,1}$
Re $(\rho^{3,1}_{3,1} - \rho^{-1,-3}_{3,1})$
Re $(\rho^{3,1}_{1,3} - \rho^{-1,-3}_{1,3})$
Re $(\rho^{3,-1}_{3,1} + \rho^{1,-3}_{3,1})$
Re $(\rho^{3,-1}_{1,3} + \rho^{1,-3}_{1,3})$
1/2 $(\rho^{3,3}_{-} - \rho^{1,1}_{-})$
0.4
0.2
0
-0.2
-0.4
0
0.1
0.2
0.3
0.4
0.5
0.6
$-t$, $(GeV/c)^2$

Fig. 5g-1

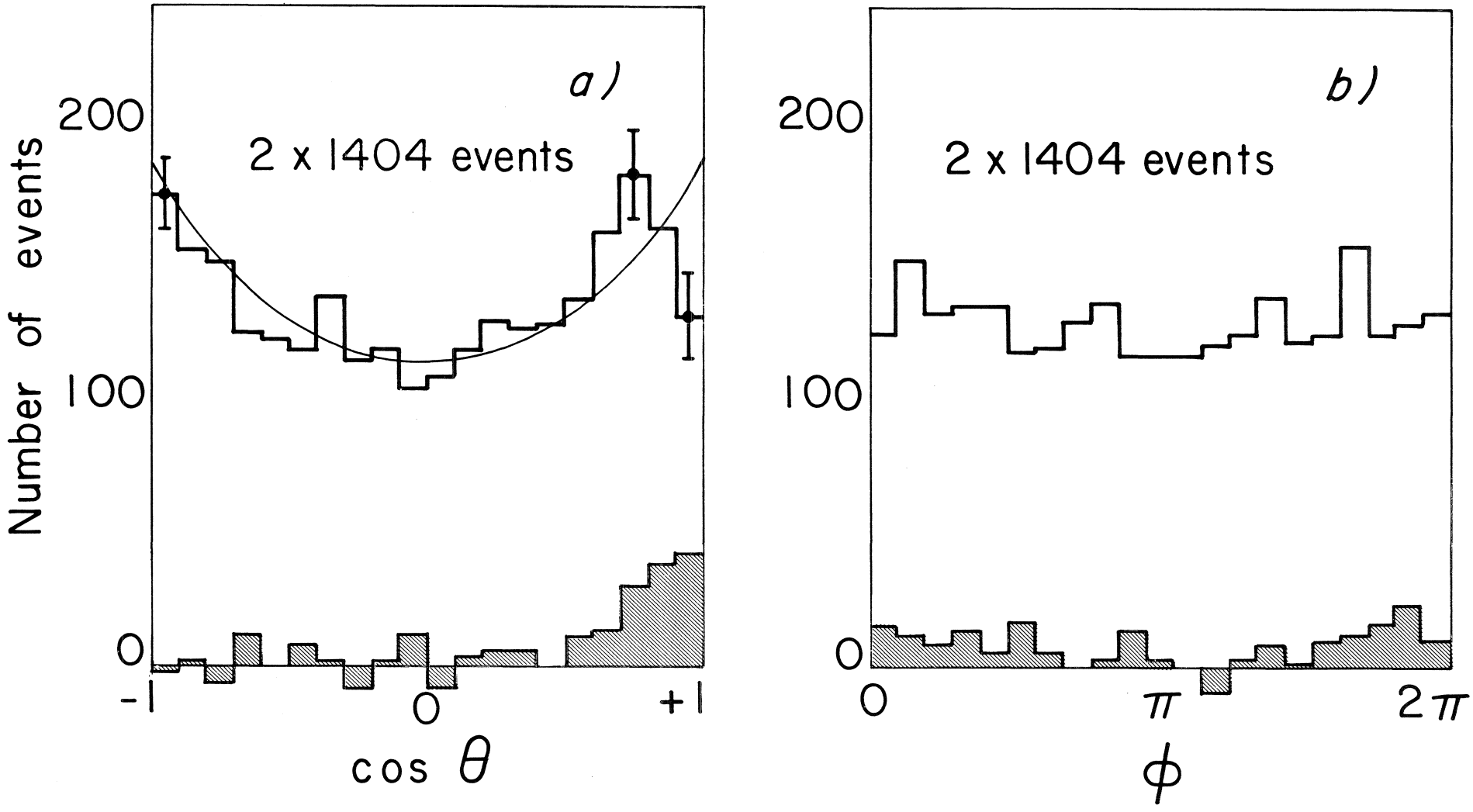
a)
2 x 1404 events
200
100
0
Number of events
-1
0
+1
cos θ
b)
2 x 1404 events
200
100
0
0
π
2π
φ

Fig. 6

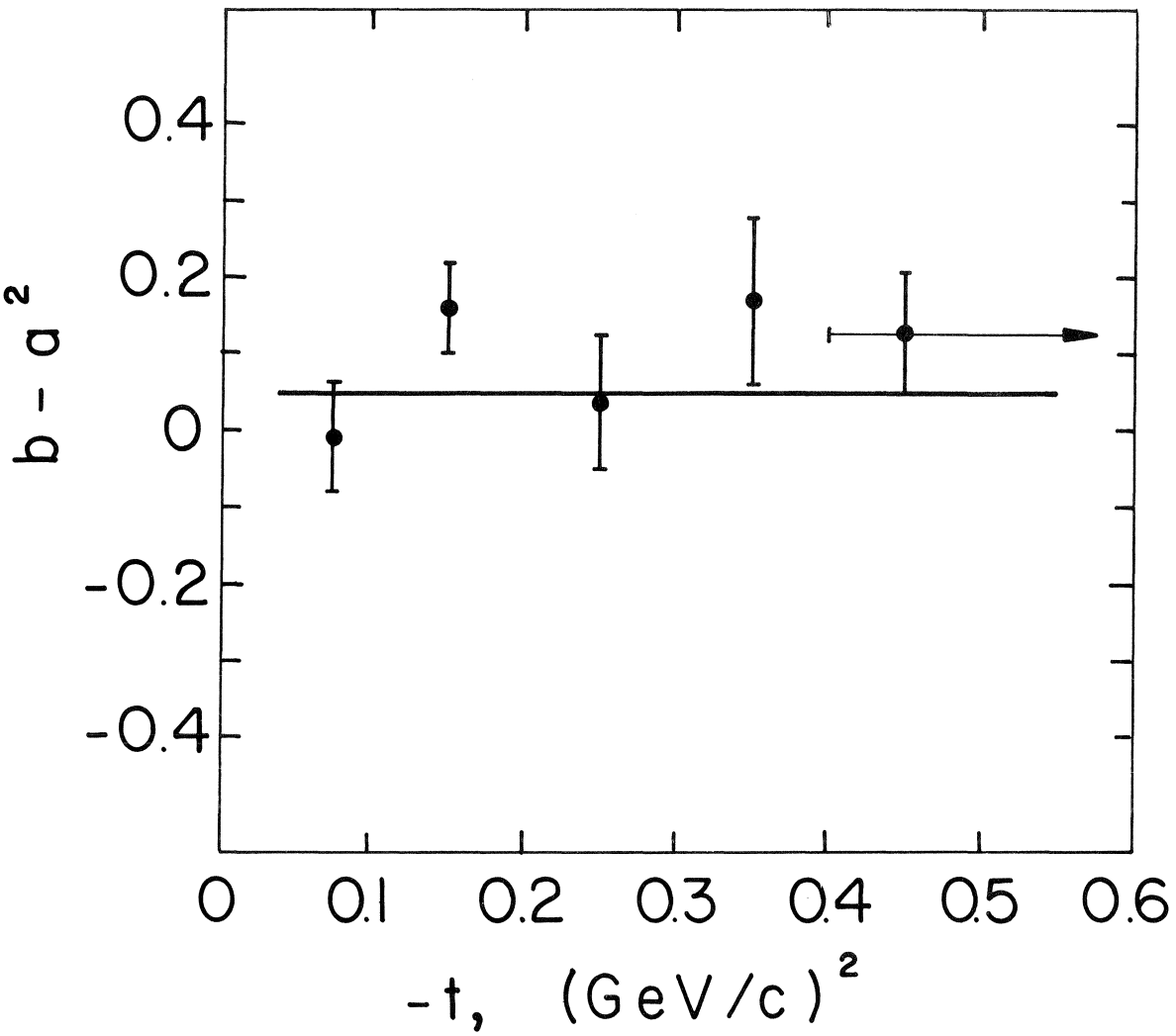

Fig. 7